Y.-H. Kuo et al. Supplemental Fig. 1

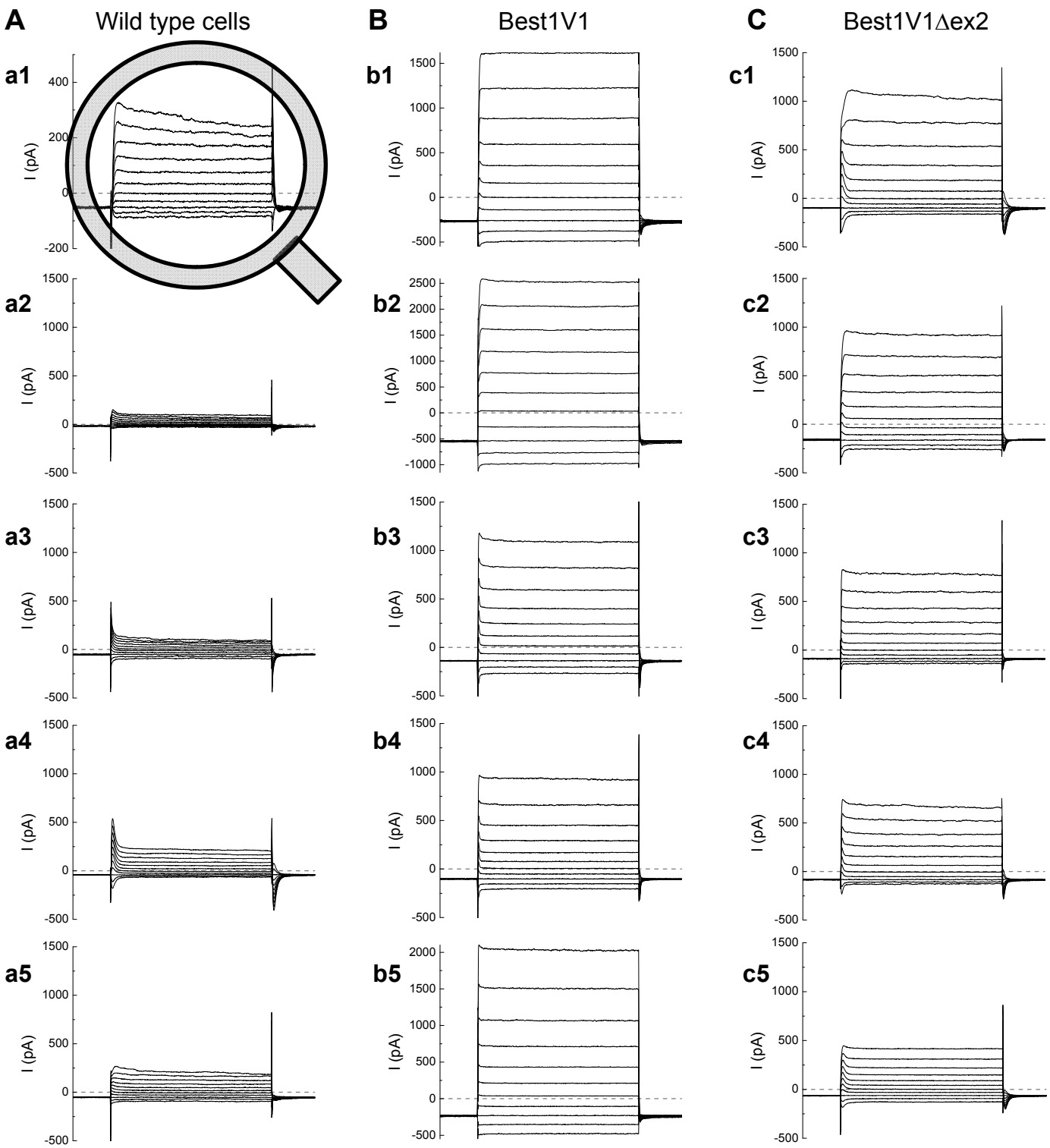

Side-by-side comparison of the whole-cell Cl^- currents recorded with $[Ca^{2+}]_{pipette}$ = 1 μM in wild type HEK293 cells (*A*) and HEK cells heteroexpressing Best1V1 (*B*) and Best1V1Δex2 (*C*).

These figures represent representtaive traces of Cl^- currents in response to step pulses from -100 mV to +100 mV in 20 mV. All currents are presented on the same scale unless indicated otherwise.

a1-a5: In the wild type cells currents were generally very small (~ 12 pA/pF). In some cells (see magnified cell in **a1**), time-dependent inactivation at positive potentials was indicative of backrgound contribution of volume-regulated anion channels. **b1-b5**: Heteroexpression of Best1V1 led to development of large (on average 75 pA/pF) Ca^{2+}-sensitive, outwardly rectifying Cl^- currents that showed no time-dependent inactivation. In **b2** and **b5** scale is expanded due to a large current magnitude. **c1-c5**: In 5 out of 12 cells transfected with Best1V1Δex2 we detected Ca^{2+}-sensitive Cl^- currents (~40 pA/pF), with strong outward rectification, and no time-dependent inactivation.

Y.-H. Kuo et al. Supplemental Fig. 2

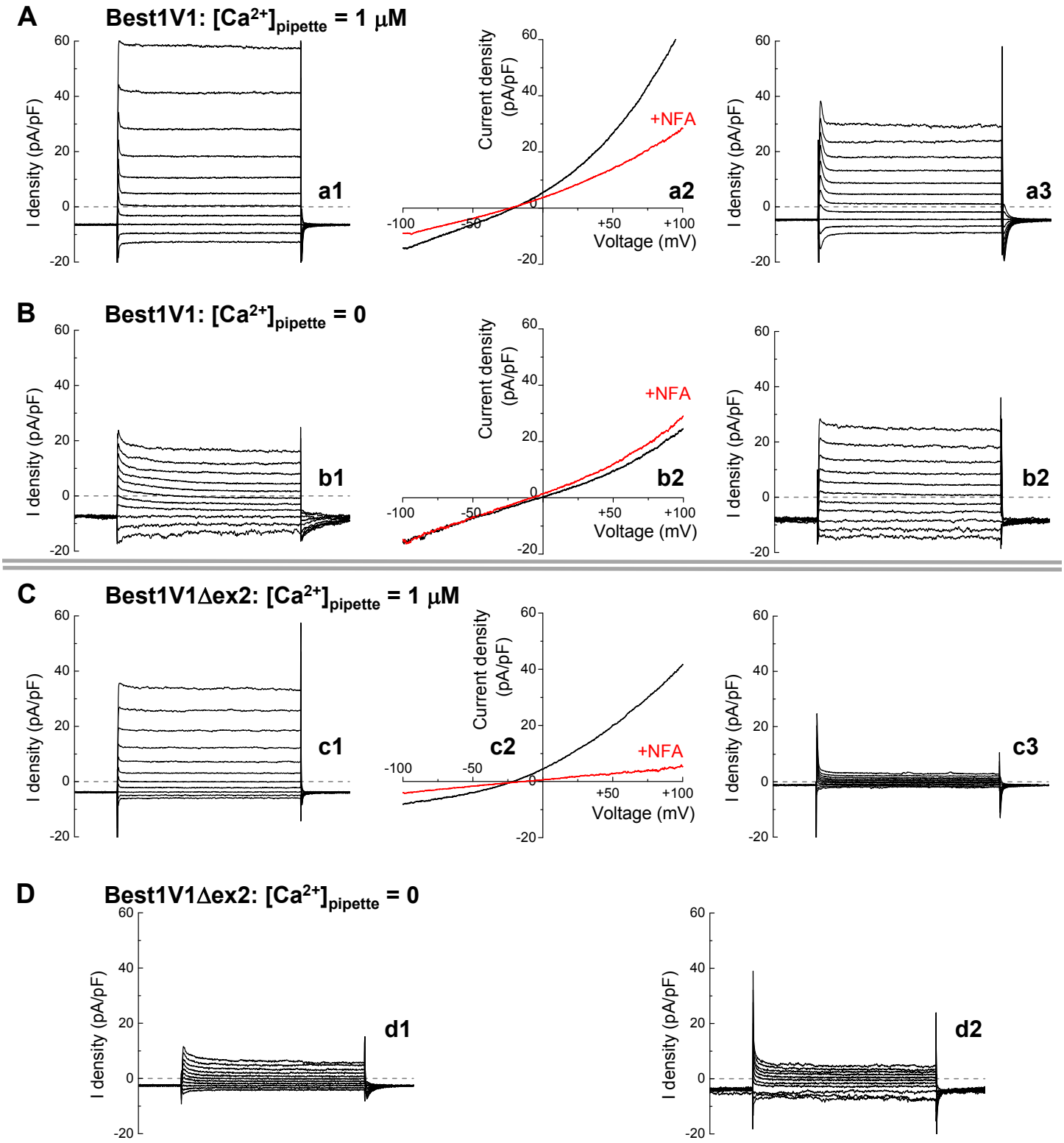

Representative traces showing Ca^{2+}- and niflumic acid sensitivity of the whole-cell Cl^- currents in HEK293 cells heteroexpressing Best1V1 (*A*, *B*) and Best1V1Δex2 (*C*, *D*).

Each series of panels shows representative currents densities (normalized to cell capacitance) in response to step pulses from -100 mV to +100 mV in 20 mV increments before (LEFT) and after (RIGHT) addition of 200 μM niflumic acid. The MIDDLE panels show I-V curves before and after addition of niflumic acid. See manuscript for discussion and additional methodological details.

Y.-H. Kuo et al. Supplemental Fig. 3

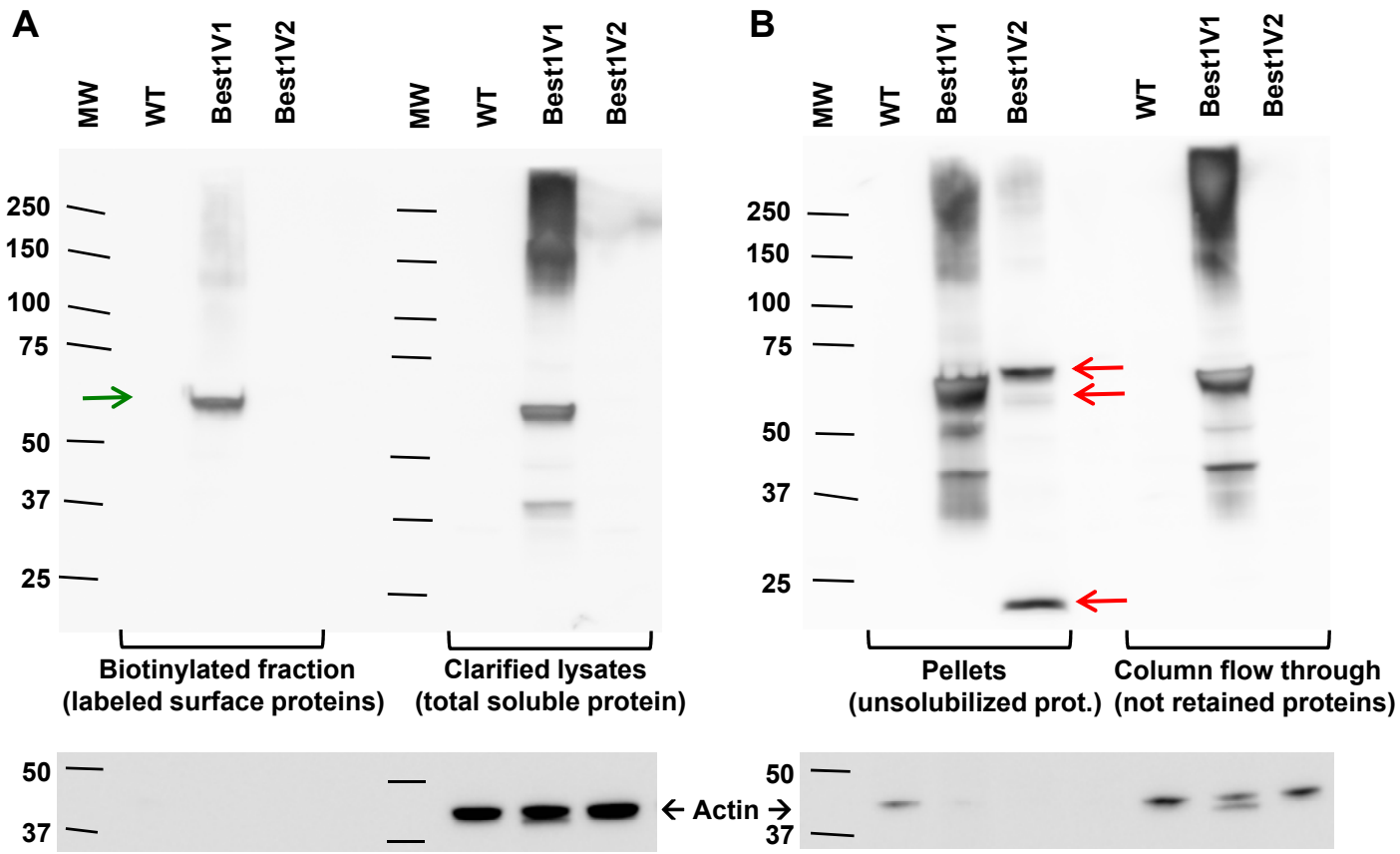

Extended analysis of the surface protein expression of Best1 splice variants using a biotinylation assay. These experiments are similar in design to those shown in Fig. 5, but additionally demonstrate that the Best1V2 protein is not solubilized under conditions of this assay, likely due to misfolding and aggregation.

A, Western blot analysis of the DDK-immunoreactivity in the precipitated biotinylated fraction (surface proteins) and clarified cell lysates (total protein load) prepared from mock transfected HEK293 cells (WT), and cells expressing Best1V1-DDK (Best1V1) and Best1V2-DDK (Best1V2). Note that the biotinylated fraction contained only one protein band with the MW close to that predicted for Best1V1 (**green arrow**). In contrast, high molecular weight aggregates and low molecular weigh degradation products were seen in clarified lysates. Lower panel shows immunoreactivity of the same membranes stripped and re-probed with the actin antibody. Note the absence of actin signal in biotinylated fraction.

B, Western blot analysis of materials left after biotinylation assay: insoluble proteins obtained after clarification of cell lysates and the flow-through proteins that have not been retained by the purification columns. **Red arrows** point to the DDK immunoreactivity in protein pellets prepared from the Best1V2-DDK overexpressing cells. These results suggest that Best1V2 forms poorly soluble aggregates and explain puzzling of absence of Best1V2 in blots presented in Fig. 5, but clear Best1V2-DDK signal after SDS solubilization seen in Fig. 2 of the main manuscript.